Published in final edited form as:
Nature. ; 483(7391): . doi:10.1038/nature10893.

Tissue factor and PAR1 promote microbiota-induced intestinal vascular remodelling

Christoph Reinhardt[1,2,3], **Mattias Bergentall**[1,2], **Thomas U. Greiner**[1,2], **Florence Schaffner**[4], **Gunnel Östergren-Lundén**[1,2], **Lars C. Petersen**[5], **Wolfram Ruf**[4], and **Fredrik Bäckhed**[1,2,6]

[1]Sahlgrenska Center for Cardiovascular and Metabolic Research/Wallenberg Laboratory, University of Gothenburg, 413 45 Gothenburg, Sweden

[2]Department of Molecular and Clinical Medicine, University of Gothenburg, 413 45 Gothenburg, Sweden

[3]Center for Thrombosis and Hemostasis (CTH), University Medical Center Mainz, Experimental Hemostaseology, 55131 Mainz, Germany

[4]Department of Immunology and Microbial Science, The Scripps Research Institute, La Jolla, California 92037, US

[5]Haemostasis Biology, DK-2760 Novo Nordisk A/S, Maalov, Denmark

[6]Novo Nordisk Foundation Center for Basic Metabolic Research, Section for Metabolic Receptology and Enteroendocrinology, Faculty of Health Sciences, University of Copenhagen, Copenhagen, DK-2200. Denmark

Abstract

The gut microbiota is a complex ecosystem that has coevolved with host physiology. Colonization of germ-free (GF) mice with a microbiota promotes increased vessel density in the small intestine[1], but little is known about the mechanisms involved. Tissue factor (TF) is the membrane receptor that initiates the extrinsic coagulation pathway[2], and it promotes developmental and tumour angiogenesis[3,4]. Here we show that the gut microbiota promotes TF glycosylation associated with localization of TF on the cell surface, the activation of coagulation proteases, and phosphorylation of the TF cytoplasmic domain in the small intestine. Anti-TF treatment of colonized GF mice decreased microbiota-induced vascular remodelling and expression of the proangiogenic factor angiopoietin-1 (Ang-1) in the small intestine. Mice with a genetic deletion of the TF cytoplasmic domain or with hypomorphic TF (*F*3) alleles had a decreased intestinal vessel density. Coagulation proteases downstream of TF activate protease-activated receptor (PAR) signalling implicated in angiogenesis[5]. Vessel density and phosphorylation of the cytoplasmic domain of TF were decreased in small intestine from PAR1-deficient ($F2r^{-/-}$) but not PAR2-deficient ($F2rl1^{-/-}$) mice, and inhibition of thrombin showed that thrombin–PAR1 signalling was upstream of TF phosphorylation. Thus, the microbiota-induced extravascular TF–PAR1 signalling

Correspondence and requests for materials should be addressed to F.B. (fredrik.backhed@wlab.gu.se).

Supplementary Information is linked to the online version of the paper at www.nature.com/nature.

Author Contributions C.R. was responsible for conception and study design, biochemical analysis of TF, analysis of vessel densities, data assembly and analysis, and writing the manuscript. M.B., T.U.G., F.S. and G.Ö.L. performed data collection, analysis and interpretation and commented on the manuscript. L.C.P. provided material. W.R. and F.B. were responsible for conception and study design, data analysis and interpretation, and writing the manuscript.

The authors declare no competing financial interests.

Readers are welcome to comment on the online version of this article at www.nature.com/nature.

loop is a novel pathway that may be modulated to influence vascular remodelling in the small intestine.

The mammalian intestine is an organ with marked postnatal vascular adaptation, which is induced at weaning and coincides with the development of an adult microbiota. In agreement with early studies showing that the gut microbiota affects vascular remodelling in the intestine[1], we showed significant increases in villus width in the small intestine of conventionally raised (CONV-R) mice in comparison with GF mice (Fig. 1a), suggesting a link between vascular remodelling and altered villus architecture on colonization. We also showed increased staining and messenger RNA levels of the vascular marker platelet–endothelial cell adhesion molecule 1 (PECAM-1) in the small intestine of both CONV-R and conventionalized (CONV-D; GF mice that had been colonized for 14 days with a normal microbiota from a CONV-R mouse) mice in comparison with GF mice (Fig. 1b–d). The increased vessel density was located to the mid-distal part of the small intestine (Supplementary Fig. 1). Staining for the tip-cell marker delta-like ligand 4 (Dll4)[6] indicated that colonization initially promoted sprouting angiogenesis but that the number of tip cells returned to basal levels once villus remodelling was complete (Fig. 1e).

We found increased levels of mRNA for Ang-1 as well as increased phosphorylation of the Ang-1 receptor Tie-2 in the small intestine of CONV-R in comparison with GF mice (Fig. 1f, g), thus providing a potential mechanism for microbiota-induced vascular remodelling. Consistent with increased vessel density, vascular endothelial growth factor receptor 1 (VEGFR-1) expression was also higher in CONV-R mice, but there were no changes in any other components of the VEGF pathway (Supplementary Fig. 2). The Ang-1–Tie-2 axis promotes the remodelling and sprouting of blood vessels[7,8]. To confirm a role for Ang-1 in microbiota-induced vascular remodelling, we injected GF mice with the specific Ang-1 inhibitor mL4-3 before and during a 14-day colonization with a normal gut microbiota and showed decreases in Tie-2 phosphorylation and intestinal vessel density (Fig. 1h–j). We identified the epithelium as a source of Ang-1, because its expression was increased in isolated primary enterocytes from CONV-R mice in comparison with those from GF mice (Fig. 1k).

Angiogenesis is linked to the cellular initiation of coagulation, and TF signalling has been shown to modulate angiogenesis[3,4]. Because bacterial components are known to stimulate the coagulation system[9], we speculated that TF could have a function in microbiota-induced angiogenesis in the intestine. In agreement with earlier studies of TF localization in humans[10] and mice[11], we identified TF predominantly in enterocytes of the villi of small intestine in both GF and CONV-R mice (Supplementary Fig. 3). We injected GF mice with anti-TF antibody or control IgG before and at 4 and 9 days after colonization with a normal caecal microbiota. Tissues were harvested 14 days after colonization, and we confirmed that the injected antibodies localized to the small intestine (Supplementary Fig. 4). Anti-TF treatment did not affect PECAM-1 staining in GF mice that were not colonized (Fig. 1l, m); neither were levels of VEGF-A, VEGFR-2 or VEGFR-3 mRNA in CONV-D mice affected (Supplementary Fig. 5). However, anti-TF treatment decreased villus width (Fig. 1n), vessel density (Fig. 1o, p) and expression of PECAM-1 and Ang-1 mRNA (Fig. 1q, r) in CONV-D mice, suggesting that TF promotes microbiota-induced remodelling of the villus vasculature. Similarly, the vessel density was decreased in intestines from mice expressing low levels of human TF (low-TF mice)[12] compared with mice expressing normal levels of human TF from a knocked-in minigene[13] (Supplementary Fig. 6). Because neither humanized mouse strain expressed alternatively spliced TF, intestinal vascular remodelling seems to be independent of alternatively spliced TF[14].

Paneth cells have been suggested to regulate microbiota-induced intestinal angiogenesis in mice, but they also have a large effect on angiogenesis independently of colonization status[1]. Anti-TF treatment did not decrease the number of Paneth cells or mRNA levels of Paneth cell-derived cryptdin 2 in CONV-D mice (Supplementary Fig. 7), indicating that treatment with antibody has no cytotoxic effect on Paneth cells. In addition, vessel density was similar in colonized CR2-*tox*176 transgenic mice, which lack Paneth cells[15], and their wild-type littermates after treatment with anti-TF (Supplementary Fig. 8).

Next we investigated whether intestinal TF expression and activity differed between GF and CONV-R mice. We did not observe any differences in intestinal levels of mRNA for TF from the two groups of mice (Fig. 2a). In contrast, immunoblot analyses identified two TF-reactive bands, one with an apparent molecular mass of 33 kDa that was present in both groups and a second band with an apparent molecular mass of 46 kDa that was present at higher levels in intestinal lysates from CONV-R and CONV-D mice (Fig. 2b, c). The gut microbiota has global effects on protein glycosylation in the small intestine[16], which is necessary for the correct cellular localization and function of many proteins including TF procoagulant activity[17]. We therefore speculated that the 46-kDa TF band resulted from microbiota-induced N-linked glycosylation of TF, the primary carbohydrate modification of TF[17]. In agreement with this, the mannose-binding lectin concanavalin A readily detected the 46-kDa form of TF in small-intestinal lysates from CONV-D mice (Supplementary Fig. 9a). Treatment with the N-glycosidase PNGase F abolished detection of the 46-kDa form and generated a partly deglycosylated form with increased electrophoretic mobility that was only weakly detected by concanavalin A. We also treated primary enterocytes from CONV-R mice with the N-glycosylation inhibitor tunicamycin and observed a decreased abundance of the 46-kDa form (Supplementary Fig. 9b, c). These findings indicate that the gut microbiota promotes N-glycosylation of TF.

Exposure of functional TF on cell surfaces is regulated by basolateral sorting in epithelial cells[18]. Surface biotinylation followed by biotin pull-down of primary enterocytes from GF mice showed that the underglycosylated TF was mainly intracellular (Fig. 2d, e). In contrast, surface labelling of proteins or carbohydrates showed that enterocytes from CONV-R mice had high levels of the fully glycosylated TF on the cell surface (Fig. 2d, e and Supplementary Fig. 10). Confocal microscopy confirmed plasma membrane localization of TF in primary enterocytes isolated from CONV-R mice (Supplementary Fig. 11 and three-dimensional reconstruction online. These changes were associated with enhanced coagulation activation, as demonstrated by increased TF–FVIIa-dependent activation of coagulation factor Xa and higher levels of thrombin–antithrombin complexes in lysates of small intestine from CONV-R in comparison with those from GF mice (Fig. 2f, g).

Not only does TF initiate coagulation, it also interacts with integrins on the extracellular side and regulates integrin function through its cytoplasmic domain[19]. Proximity ligation and immunoprecipitation experiments showed increased TF–β_1 integrin complex formation in intestinal tissue from CONV-R mice in comparison with GF counterparts (Supplementary Fig. 12a, b). Furthermore, TF–β_1 integrin complex formation was decreased by treating CONV-R mice with tunicamycin (Supplementary Fig. 12c). The cytoplasmic domain of TF contains a conserved Ser/Thr-Pro phosphorylation site[20]. Phosphorylation of this domain has been observed at sites of neovascularization[4]; it requires surface localization of TF[21] and regulates integrin function[19]. An antibody directed against the phosphorylated domain of mouse TF detected increased phosphorylation in the 46-kDa form of TF in lysates of small intestine from CONV-R in comparison with that from GF mice (Fig. 3a), and treatment of primary enterocytes from CONV-R mice with tunicamycin decreased levels of the phosphorylated 46-kDa form of TF (Fig. 3b, c).

To test directly whether the TF cytoplasmic domain was involved in vascular remodelling, we analysed small-intestinal tissue from mice with a targeted deletion of this domain (ΔCT mice)[22] and age-matched wild-type mice. ΔCT mice had significantly decreased villus vascularization (Fig. 3d, e) and decreased expression of mRNA for PECAM-1 and Ang-1 in comparison with wild-type mice (Fig. 3f). TF from wild-type and ΔCT mice had similar electrophoretic mobilities (Supplementary Fig. 13). These data show that the TF cytoplasmic domain has a function in increasing vessel density in the small intestine but that it is not required for glycosylation. Anti-TF treatment decreased TF phosphorylation but not total TF levels in CONV-D mice (Supplementary Fig. 14). These results indicate that the inhibitory effects of anti-TF on vascular remodelling are independent of TF downregulation but, at least in part, involve inhibition of TF cytoplasmic domain phosphorylation.

TF also mediates signalling through coagulation proteases that activate the G-protein-coupled receptors PAR1 and PAR2 (refs 4, 5). We investigated the effect of the gut microbiota on PAR expression in small-intestinal tissue. Levels of mRNA for PAR1 but not those for PAR2 were increased in CONV-R mice in comparison with GF counterparts (Fig. 4a). PAR1 is abundantly expressed in endothelial cells[5], but we found that PAR1 was also expressed in enterocytes and at higher levels in cells from CONV-R mice than in GF counterparts (Supplementary Fig. 15). PECAM-1 staining (Fig. 4b, c) as well as levels of mRNA for PECAM-1 and Ang-1 (Fig. 4d, e) were decreased in intestinal tissue from PAR1-deficient (*F2r*$^{-/-}$) but not PAR2-deficient (*F2rl1*$^{-/-}$) mice, which is in agreement with a recent study showing that thrombin induces PAR1-dependent Ang-1 expression in endothelial cells[23]. Together, these data show that the microbiota induces increased expression of PAR1, and that PAR1 has a role in remodelling the vasculature in the small intestine.

We next investigated the potential interrelation between PAR1 and TF in intestinal tissue. Phosphorylation of TF was decreased in lysates of small intestine from *F2r*$^{-/-}$ in comparison with that from wild-type and *F2rl1*$^{-/-}$ mice (Fig. 4f), indicating that PAR1 acts upstream of TF phosphorylation. We blocked thrombin and thrombin-dependent PAR1 signalling with hirudin immediately before and during colonization of GF mice for 6 h, and observed a striking decrease in TF phosphorylation in lysates of small intestine (Fig. 4g, h). We also showed that thrombin increased the phosphorylation of TF in primary enterocytes (Fig. 4i, j). Taken together, these data suggest that functional, procoagulant TF is required for the generation of thrombin, which in turn activates PAR1 to promote phosphorylation of the cytoplasmic domain of TF in enterocytes.

This study has uncovered a novel connection between TF, PAR1 and Ang-1 in modulating vascular remodelling after colonization. Our results support a model in which the microbiota induces increased glycosylation and surface localization of TF in the small intestine, leading to activation of coagulation, PAR1-dependent-phosphorylation of the TF cytoplasmic domain, and TF cytoplasmic domain signalling linked to Ang-1-dependent vascular remodelling (Supplementary Fig. 16). This pathway is distinct from established models of ocular angiogenesis[4] or tumour-induced neovascularization, which requires the TF–Factor VIIa–PAR2-mediated induction of pro-angiogenic chemokines[24]. We therefore suggest that TF may support distinct pro-angiogenic pathways in different tissues. Increased vascularization of the villi of the small intestine increases oxygenation of the villi, which are shortened and widened after colonization. This process may promote increased nutrient absorption, which has been associated with increased adiposity in CONV-R mice[25]. Further dissection of how TF and PAR1 mediate postnatal microbiota-induced angiogenesis may provide new therapeutic targets for improving intestinal homeostasis and modulating the absorptive capacity of the gut.

METHODS

Administration of mL4-3

mL4-33 (ref. 30) (2.32 mg per kg body weight) was administered subcutaneously to GF mice before conventionalization with a caecal microbiota from a CONV-R donor. Additional injections of mL4-3 were given three times a week. The mice were killed 14 days after colonization.

Preparation of intestinal samples

For immunohistochemistry and *in situ* hybridization, the small intestine (divided into eight equal segments) and colon were flushed with PBS after excision and opened longitudinally. The tissue was fixed overnight in 4% formaldehyde at 4 °C, washed three times in PBS, and incubated in 10% sucrose in PBS at 4 °C. After 3 h, the buffer was replaced with 20% sucrose and 10% glycerol in PBS, and the tissue was incubated at 4 °C overnight. Tissues were dried with a paper towel and mounted in OCT on solid CO_2. Frozen sections 6 μm thick were prepared.

For mRNA analyses, the segments were frozen immediately at −80 °C in liquid nitrogen. For immunoblots, the fifth segment was flash-frozen and homogenized for 10 min in lysis buffer (50 mM Tris-HCl pH 8, 150 mM NaCl, 5 mM EDTA, 1% Triton X-100) containing Roche Complete protease and PhosStop phosphatase inhibitors (diluted 1:10). The homogenate was incubated for 30 min on ice and centrifuged three times at 9,000*g* for 10 min to remove insoluble cell debris.

Immunohistochemistry

Sections were incubated for 20 min at room temperature and blocked for 1 h with diluted TBST (50 mM Tris-HCl pH 7.5, 150 mM NaCl, 0.1% Triton X-100) containing 5% rabbit serum. The blocking solution was removed and the following primary antibodies, diluted in the same blocking solution, were added: rat anti-mouse PECAM-1 (dilution 1:300; BD, Franklin Lakes), chicken anti-cytokeratin 8 (dilution 1:100; Abcam, Cambridge), goat-anti DLL4 (dilution 1:50; R&D), rabbit anti-mouse TF[29] (1 μg ml^{-1}) and rabbit anti-PAR1 (dilution 1:300; Sigma). The samples were incubated overnight at 4 °C, washed three times for 5 min in TBST and incubated for 1 h with secondary antibodies (Invitrogen, Carlsbad) at room temerature (rabbit anti-rat Alexa594, dilution 1:800; goat anti-rabbit IgG Alexa488, dilution 1:5,000; goat anti-chicken IgG Alexa488, dilution 1:2,000; all from BD). Nuclei were stained with Hoechst dye (3 μg ml^{-1}; Sigma) and the sections were washed three times for 10 min in TBST. For detection of Paneth cells, fluorescein isothiocyanate-isolectin (10 μg ml^{-1}; Sigma) was used. Slides were mounted, and viewed at ×20 and ×40 magnification with a fluorescence microscope (Axioplan 2 imaging; Zeiss, Oberkochen). Biopix iQ software (http://www.biopix.se) was used to quantify PECAM-1 staining in 2–11 villi per mouse. Confocal images and three-dimensional reconstructions were obtained with a Leica TCS SP5 confocal microscope (Leica, Wetzlar).

Quantitative reverse transcriptase polymerase chain reaction (qRT–PCR) analysis

Total RNA was isolated from small-intestinal tissues and isolated primary enterocytes with the RNeasy kit (Qiagen, Hilden). Total RNA (0.5 μg) was reverse transcribed (High Capacity cDNA Reverse Transcription kit; Applied Biosystems, Foster City) and SYBR green-based qRT–PCR was performed as described previously[31]. Primers are listed in Supplementary Table 1.

In situ hybridization

Mouse TF cDNA[32] was subcloned into pSPT19 for subsequent *in vitro* RNA synthesis. Non-radioactive, digoxigenin-labelled sense and antisense RNA probes were synthesized with the DIG RNA Labelling Kit (SP6/T7; Roche, Mannheim). Tissues were pretreated for 2 min with proteinase K (10 μg ml^{-1}) in 50 mM Tris-HCl pH 7.5, 5 mM EDTA; the reaction was stopped by washing for 30 s in 0.2% glycine in PBS, followed by two additional washing steps in PBS. Tissues were fixed for 15 min in 4% paraformaldehyde in PBS, and washed in PBS for 2 min. Hybridization solution was added, and tissues were pre-hybridized for 1 h at 65 °C. RNA probe (8 ng μl^{-1} hybridization solution) was added and preheated for 5 min at 80 °C; 100 μl was added to each slide and incubated overnight at 65 °C in a humidified box. Slides were washed three times for 30 min in a preheated washing solution at 65 °C and twice for 30 min in MABT (100 mM maleic acid pH 7.5, 150 mM NaCl, 0.1% Tween 20) at room temperature. Slides were blocked with 2% blocking reagent (Roche, Mannheim), 20% heat-inactivated sheep serum (Sigma) in MABT for 1 h at room temperature. Binding of the RNA template was detected with alkaline-phosphatase-conjugated Fab fragments (Roche, Mannheim) and BM Purple.

Factor Xa activity

Factor Xa activity was measured in small-intestinal lysates as described previously[32].

Measurement of TAT complexes

The TAT ELISA Kit (Uscnlife, Guangguguoji) was used for determination of the concentration of mouse TAT complexes in lysates of small-intestinal tissue.

Immunoprecipitation

Tissue lysates were incubated for 1 h with anti-mouse TF antibody (70 μg ml^{-1}; American Diagnostica, Stamford) or anti-integrin β_1 antibody (dilution 1:100l Cell Signaling, Danvers), and immunocomplexes were precipitated by adding 50 μl of Protein A-Sepharose fast flow 4B (Sigma). TF and integrin β_1 antigen were detected as described below.

Glycosidase treatment

Anti-TF precipitates were boiled for 5 min to release the captured antigen from the antibody. Samples were cooled to 4 °C, and 20 U ml^{-1} peptide N-glycosidase F (Sigma) was added for 90 min at 37 °C and then boiled again for 5 min to inactivate the glycosidase. Treatment with O-glycosidase (25 mU ml^{-1}; Merck, Darmstadt) was performed for 3 h at 37 °C.

Immunoblotting

Tissue lysates or immunoprecipitates were separated by using a NuPAGE system with MOPS buffer and 10% BisTris gels. Proteins were transferred to poly(vinylidene difluoride) membranes (Invitrogen, Carlsbad). The membrane was blocked in 5% milk powder (in PBS/Tween) and incubated for 1.5 h in 5% milk powder containing the primary antibody (rabbit anti-mouse TF (2.5 μg ml^{-1}; American Diagnostica, Stamford) for immunoprecipitation, rabbit anti-mouse TF and rabbit anti-mouse phospho-TF (2 μg ml^{-1}) for specificity controls —see Supplementary Fig. 17, rabbit anti-integrin β_1 (dilution 1:1,000; Cell Signaling), rabbit anti-actin (dilution 1:200; Sigma), rabbit anti- phospho-Tie2 (dilution 1:250; R&D) and rabbit anti-Tie-2 antibody (dilution 1:250; Abcam)). Secondary goat anti-rabbit IgG (horseradish peroxidase-conjugated; Santa Cruz Biotechnology, Santa Cruz) was applied for 1 h. Alternatively, the membrane was incubated with horseradish peroxidase-conjugated concanavalin A (Sigma) to detect sugar moieties after immunoprecipitation. Then the membrane was first washed for 2 min with PBS and incubated overnight with the lectin

solution (PBS containing Mg^{2+} and Ca^{2+}). The next day, the blot was rinsed three times with PBS/Tween. Blots were developed with enhanced chemiluminescence solutions (Amersham Biosciences, Little Chalfont). For densitometric analysis of protein bands, the software Multi Gauge V3.0 (Fuji Film, Tokyo) was applied.

Cell-surface labelling and pull-down with *N*-hydroxysuccinimido-biotin

For amine-reactive biotinylation and isolation of cell surface proteins from isolated primary enterocytes, the Cell Surface Protein Isolation Kit (Pierce, Rockford) was used. Isolated proteins were separated on a 10% BisTris gel (Invitrogen), and TF antigen was analysed by immunoblotting.

Proximity ligation assay[33]

Slides with adhering primary enterocytes were blocked and incubated with primary antibodies (monoclonal rat-anti-mouse TF (1H1)[34], 23.4 μg ml^{-1}, provided by Daniel Kirchhofer; rabbit polyclonal anti-integrin β_1, dilution 1:50; Cell Signaling Technology). Secondary antibodies (anti-rat and anti-rabbit) conjugated with unique DNA probes (Olink Bioscience, Uppsala) were added. Slides were evaluated with a Leica TCS SP5 confocal microscope. If TF and integrin β_1 antigens are closer than 30 nm, a fluorescence signal can be generated.

Supplementary Material

Refer to Web version on PubMed Central for supplementary material.

Acknowledgments

We thank R. Perkins for editing the manuscript; C. Arvidsson, A. Hallén, S. Wagoner, M. Karlsson, D. O'Donell, S. Islam, N. Hörmann and A. Mohammadzadeh for technical assistance; A. Hallén for providing Supplementary Fig. 16; and P. Lindahl, J. Gordon, C. Betsholtz, M. Bergö, A. Wichmann, V. Tremaroli, M. Levin and S. Massberg for comments and suggestions. We are grateful to D. Kirchhofer for the gift of 1H1 monoclonal anti-mouse TF antibody, J. Nichols at Amgen for mL4-3, N. Mackman for the low-TF mice, M. Anderson for the human TF knock-in mice, and J. Gordon for providing CR2-*tox*176 mice. This study was supported by the Swedish Foundation for Strategic Research, the Swedish Research Council, Torsten and Ragnar Söderberg's foundation, Petrus and Augusta Hedlund's foundation, and the Swedish federal government under the LUA/ALF agreement to F.B., National Institutes of Health grants HL-60742 and HL-77753 to W.R., and a Marie Curie Fellowship, a Marie Curie Reintegration Grant from the European Union and the German Federal Ministry of Education and Research (BMBF 01EO1003) to C.R.

References

1. Stappenbeck TS, Hooper LV, Gordon JI. Developmental regulation of intestinal angiogenesis by indigenous microbes via Paneth cells. Proc Natl Acad Sci USA. 2002; 99:15451–15455. [PubMed: 12432102]
2. Morrissey JH, Fakhrai H, Edgington TS. Molecular cloning of the cDNA for tissue factor, the cellular receptor for the initiation of the coagulation protease cascade. Cell. 1987; 50:129–135. [PubMed: 3297348]
3. Carmeliet P, et al. Role of tissue factor in embryonic blood vessel development. Nature. 1996; 383:73–75. [PubMed: 8779717]
4. Belting M, et al. Regulation of angiogenesis by tissue factor cytoplasmic domain signaling. Nature Med. 2004; 10:502–509. [PubMed: 15098027]
5. Griffin TC, Srinivasan Y, Zheng YW, Huang W, Coughlin SR. A role for thrombin receptor signaling in endothelial cells during embryonic development. Science. 2001; 293:1666–1670. [PubMed: 11533492]
6. Hellström M, et al. Dll4 signalling through Notch 1 regulates formation of tip cells during angiogenesis. Nature. 2007; 445:776–780. [PubMed: 17259973]

7. Sato TN, et al. Distinct roles of the receptor tyrosine kinases Tie-1 and Tie-2 in blood vessel formation. Nature. 1995; 376:70–74. [PubMed: 7596437]
8. Suri C, et al. Requisite role of angiopoietin-1, a ligand for the TIE2 receptor, during embryonic angiogenesis. Cell. 1996; 87:1171–1180. [PubMed: 8980224]
9. Iwanaga S. The limulus clotting reaction. Curr Opin Immunol. 1993; 5:74–82. [PubMed: 8452677]
10. More L, et al. Immunohistochemical study of tissue factor expression in normal intestine and idiopathic inflammatory bowel disease. J Clin Pathol. 1993; 46:703–708. [PubMed: 8408693]
11. Luther T, et al. Tissue factor expression during human and mouse development. Am J Pathol. 1996; 149:101–113. [PubMed: 8686734]
12. Parry GC, Erlich JH, Carmeliet P, Luther T, Mackman N. Low levels of tissue factor are compatible with development and hemostasis in mice. J Clin Invest. 1998; 101:560–569. [PubMed: 9449688]
13. Snyder LA, et al. Expression of human tissue factor under the control of the mouse tissue factor promoter mediates normal hemostasis in knock-in mice. J Thromb Haemost. 2008; 6:306–314. [PubMed: 18005233]
14. van den Berg YW, et al. Alternatively spliced tissue factor induces angiogenesis through integrin ligation. Proc Natl Acad Sci USA. 2009; 106:19497–19502. [PubMed: 19875693]
15. Garabedian EM, Roberts LJ, McNevin MS, Gordon JI. Examining the role of Paneth cells in the small intestine by lineage ablation in transgenic mice. J Biol Chem. 1997; 272:23729–23740. [PubMed: 9295317]
16. Bry L, Falk PG, Midtvedt T, Gordon JI. A model of host–microbial interactions in an open mammalian ecosystem. Science. 1996; 273:1380–1383. [PubMed: 8703071]
17. Krudysz-Amblo J, Jennings ME II, Mann KG, Butenas S. Carbohydrates and activity of natural and recombinant tissue factor. J Biol Chem. 2010; 285:3371–3382. [PubMed: 19955571]
18. Camerer E, et al. Opposite sorting of tissue factor in human umbilical vein endothelial cells and Madin–Darby canine kidney epithelial cells. Blood. 1996; 88:1339–1349. [PubMed: 8695852]
19. Dorfleutner A, Hintermann E, Tarui T, Takada Y, Ruf W. Cross-talk of integrin α3β1 and tissue factor in cell migration. Mol Biol Cell. 2004; 15:4416–4425. [PubMed: 15254262]
20. Zioncheck TF, Soumitra R, Vehar GA. The cytoplasmic domain of tissue factor is phosphorylated by a protein kinase C-dependent mechanism. J Biol Chem. 1992; 267:3561–3564. [PubMed: 1740409]
21. Dorfleutner A, Ruf W. Regulation of tissue factor cytoplasmic domain phosphorylation by palmitoylation. Blood. 2003; 102:3998–4005. [PubMed: 12920028]
22. Melis E, et al. Targeted deletion of the cytoplasmic domain of tissue factor in mice does not affect development. Biochem Biophys Res Commun. 2001; 286:580–586. [PubMed: 11511099]
23. Blackburn JS, Brinckerhoff CE. Matrix metalloproteinase-1 and thrombin differentially activate gene expression in endothelial cells via PAR-1 and promote angiogenesis. Am J Pathol. 2008; 173:1736–1746. [PubMed: 18988801]
24. Schaffner F, et al. Cooperation of tissue factor cytoplasmic domain and PAR2 signaling in breast cancer development. Blood. 2010; 116:6106–6113. [PubMed: 20861457]
25. Bäckhed F, et al. The gut microbiota as an environmental factor that regulates fat storage. Proc Natl Acad Sci USA. 2004; 101:15718–15723. [PubMed: 15505215]
26. Connolly AJ, Ishihara H, Kahn ML, Farese RV Jr, Coughlin SR. Role of the thrombin receptor in development and evidence for a second receptor. Nature. 1996; 381:516–519. [PubMed: 8632823]
27. Damiano BP, et al. Cardiovascular responses mediated by protease-activated receptor-2 (PAR-2) and thrombin receptor (PAR-1) are distinguished in mice deficient in PAR-2 or PAR-1. J Pharmacol Exp Ther. 1999; 288:671–678. [PubMed: 9918574]
28. Perreault N, Beaulieu JF. Primary cultures of fully differentiated and pure human intestinal epithelial cells. Exp Cell Res. 1998; 245:34–42. [PubMed: 9828099]
29. Furlan-Freguia C, Marchese P, Gruber A, Ruggeri ZM, Ruf W. P2X7 receptor signaling contributes to tissue factor-dependent thrombosis in mice. J Clin Invest. 2011; 121:2932–2944. [PubMed: 21670495]

30. Falcón BL, et al. Contrasting actions of selective inhibitors of angiopoietin-1 and angiopoietin-2 on the normalization of tumor blood vessels. Am J Pathol. 2009; 175:2159–2170. [PubMed: 19815705]

31. Stappenbeck TS, et al. Laser capture microdissection of mouse intestine: characterizing mRNA and protein expression, and profiling intermediary metabolism in secified cell populations. Methods Enzymol. 2002; 356:167–196. [PubMed: 12418197]

32. Petersen LC, et al. Characterization of recombinant murine factor VIIa and recombinant murine tissue factor: a human–murine species compatibility study. Thromb Res. 2005; 116:75–85. [PubMed: 15850611]

33. Söderberg O, et al. Direct observation of individual endogenous protein complexes *in situ* by proximity ligation. Nature Methods. 2006; 3:995–1000. [PubMed: 17072308]

34. Kirchhofer D, Moran P, Bullens S, Peale F. A monoclonal antibody that inhibits mouse tissue factor function. J Thromb Haemost. 2005; 3:1098–1099. [PubMed: 15869619]

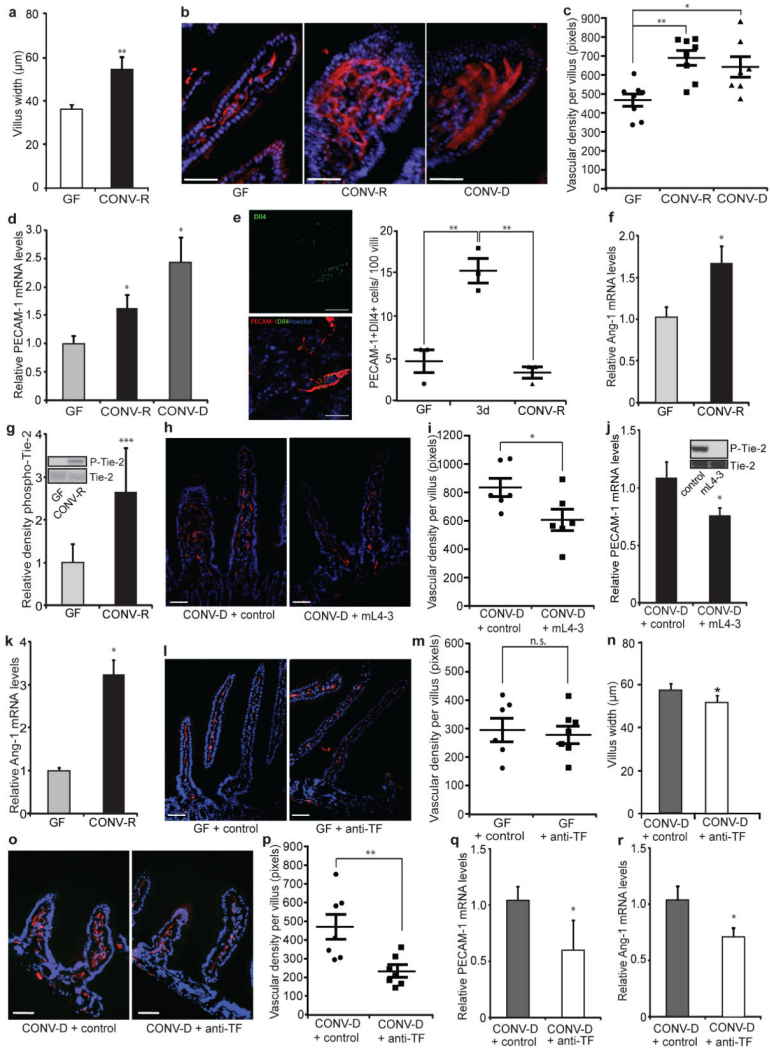

Figure 1. TF promotes microbe-induced vascular remodelling in the gut

a, Villus width of sections of small intestine from GF and CONV-R mice (*n* = 4 mice per group). **b**, PECAM-1 staining (red) of sections of small intestine from GF, CONV-R and CONV-D mice. Nuclei were stained with Hoechst nuclear dye (blue). **c**, Quantification of **b** (*n* = 7 or 8 mice per group). **d**, Relative levels of mRNA for the vascular marker PECAM-1 in GF, CONV-R and CONV-D mice (*n* = 6 or 7 mice per group). **e**, Dll4 staining (green) of sections of small intestine from GF, ex-GF mice colonized for 3 days (3d), and CONV-R mice. Endothelial cells were stained with PECAM-1 (red). Dll4-positive endothelial cells per 100 villi were quantified (*n* = 3 mice per group). **f**, Relative levels of mRNA for Ang-1 in sections of small intestine from GF and CONV-R mice (*n* = 7–11 mice per group). **g**, Anti-phospho-Tie-2 immunoblot (Y1100 phosphorylation site) and quantification relative to total Tie-2 of small-intestinal lysates from GF and CONV-R mice (*n* = 5 mice per group). **h**, PECAM-1 staining of sections of small intestine from mice treated with control NaCl solution or the Ang-1 neutralizing peptibody mL4-3. **i**, Quantification of **h** (*n* = 6 mice per group). **j**, Relative levels of mRNA for PECAM-1 in sections of small intestine from CONV-D mice treated with NaCl control or mL4-3 (*n* = 10 or 11 mice per group). The inset shows that mL4-3 is a potent inhibitor of Ang-1-mediated Tie-2 phosphorylation. **k**, Relative levels of mRNA for Ang-1 in primary enterocytes from GF and CONV-R mice (*n* =

10 or 11 mice per group). **l**, PECAM-1 staining of sections of small intestine from GF mice treated with control or anti-TF antibody. **m**, Quantification of **l** (*n* = 6 or 7 mice per group). **n**, Villus width of sections of small intestine from CONV-D mice treated with control or anti-TF antibody (*n* = 4 mice per group). **o**, PECAM-1 staining of sections of small intestine from CONV-D mice treated with control or anti-TF antibody. **p**, Quantification of **o** (*n* = 7 mice per group). **q**, **r**, Relative levels of mRNA for PECAM-1 (**q**) and Ang-1 (**r**) in small intestine from CONV-D mice treated with control or anti-TF antibody (*n* = 5 or 6 mice per group). Female Swiss Webster mice or cells isolated from these mice were analysed in all panels. Scale bars, 50 μm. Results are shown as means ± s.e.m. Asterisk, $P < 0.05$; two asterisks, $P < 0.01$; three asterisks, $P < 0.005$; n.s., not significant.

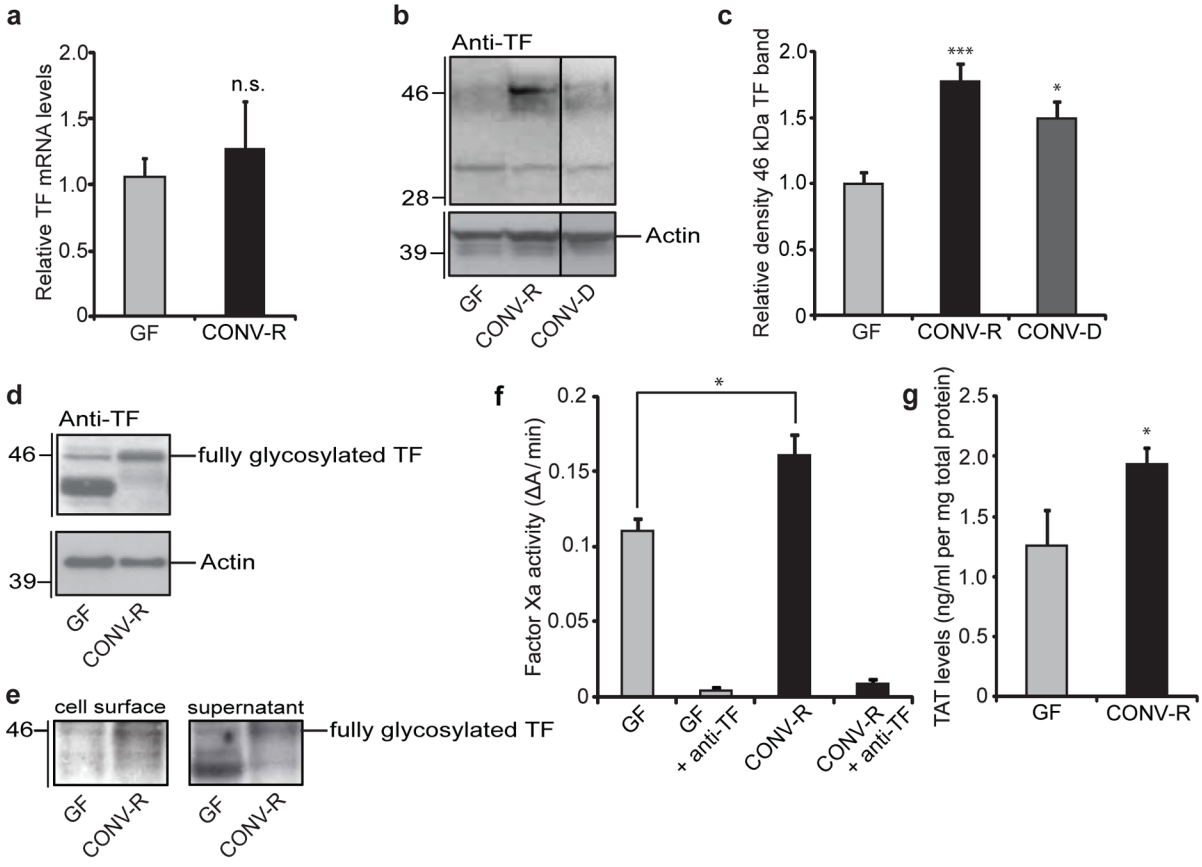

Figure 2. The gut microbiota increases TF procoagulant activity and cell-surface localization

a, Relative levels of mRNA for TF in sections of small intestine from GF and CONV-R mice (n = 7–11 mice per group). **b**, Anti-TF immunoblot of small-intestinal lysates from GF, CONV-R and CONV-D mice. **c**, Quantification of the 46-kDa TF band shown in **b** (n = 14–25 mice per group). Data are normalized to actin and expressed relative to GF. **d**, Anti-TF immunoblot of primary enterocytes (from GF and CONV-R mice) after 2 h of culture. **e**, Anti-TF immunoblots from *N*-hydroxysuccinimido-biotin-labelled primary enterocytes from GF and CONV-R mice. Left: pull-down of proteins located on the plasma membrane with NeutrAvidin beads. Right: supernatant containing unlabelled proteins. **f**, Factor Xa activity in small-intestinal lysates from GF and CONV-R mice treated with control or anti-TF antibody (n = 4 or 5 mice per group). **g**, Levels of thrombin–antithrombin (TAT) complexes in small-intestinal lysates from GF and CONV-R mice (n = 7 mice per group). Female Swiss Webster mice or cells isolated from these mice were analysed in all panels. Results are shown as means ± s.e.m. Asterisk, $P < 0.05$; three asterisks, $P < 0.005$; n.s., not significant.

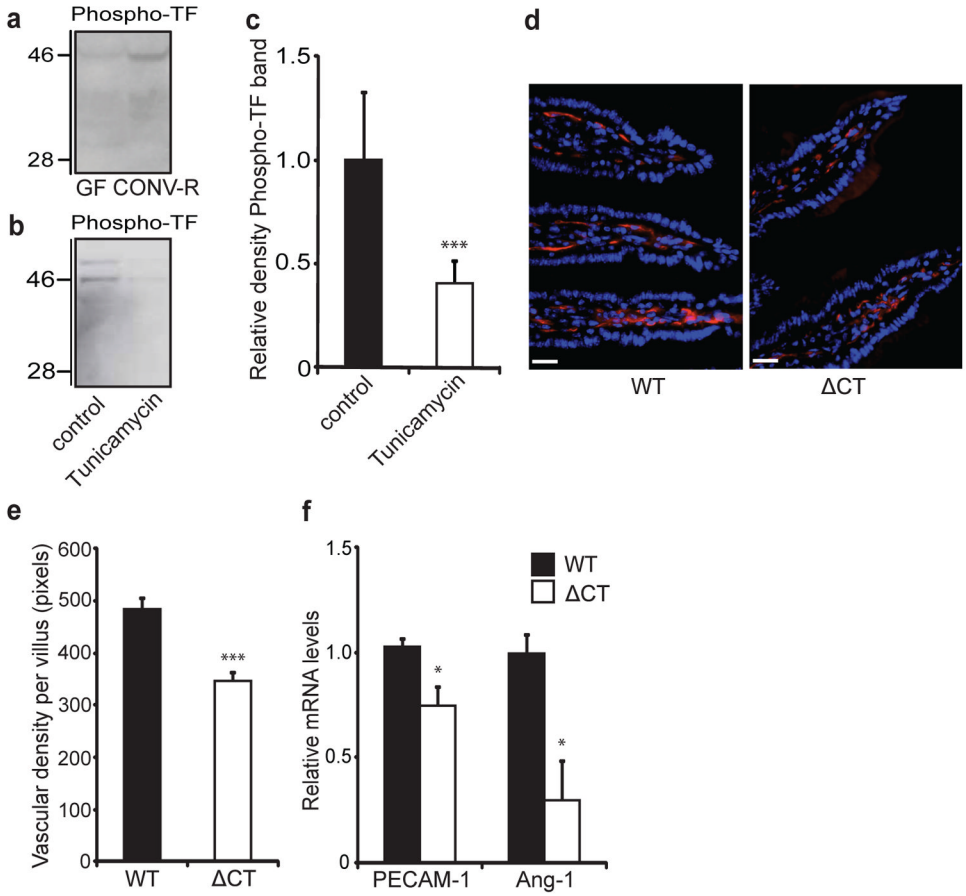

Figure 3. The gut microbiota increases phosphorylation of the cytoplasmic tail of TF, which increases vessel density in the intestine

a, **b**, Anti-phospho-TF immunoblot of (**a**) small-intestinal lysates from GF and CONV-R mice and (**b**) primary enterocytes (from CONV-R mice) incubated for 2 h in the absence and presence of tunicamycin (10 μmol l^{-1}). **c**, Quantification of **b** (n = 5 mice per group). **d**, PECAM-1 staining (red) of sections of small intestine from 10–12-week-old wild-type (WT) and ΔCT female mice on a C57Bl6/J genetic background. Nuclei were stained with Hoechst nuclear dye (blue). **e**, Quantification of **d** (n = 4–6 mice per group). **f**, Relative levels of mRNA for PECAM-1 and Ang-1 in segments of small intestine from WT and ΔCT mice (n = 3 or 4 mice per group). Female Swiss Webster mice or cells isolated from these mice were analysed in **a–c**. Scale bars, 20 μm. Results are shown as means ± s.e.m. Asterisk, $P < 0.05$; three asterisks, $P < 0.005$.

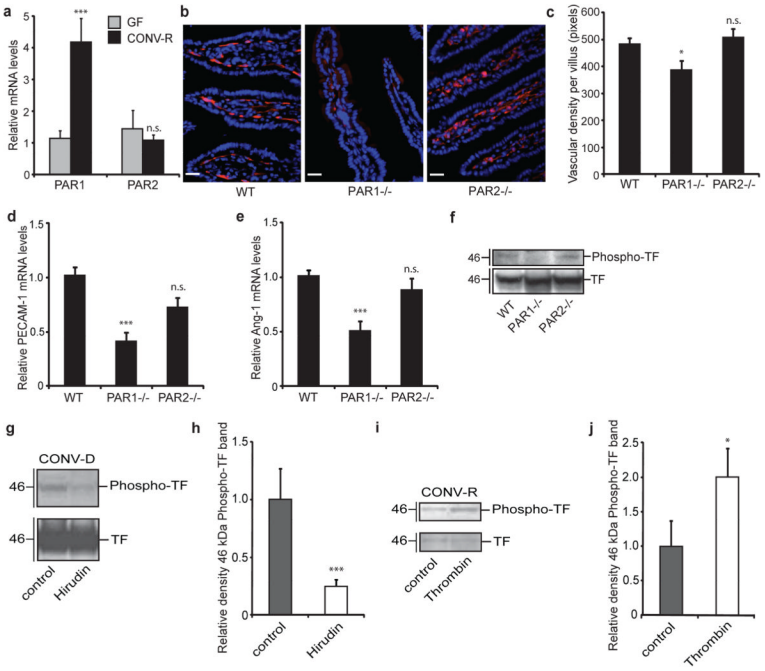

Figure 4. PAR1 activation increases vessel density in the small intestine

a, Relative levels of mRNA for PAR1 and PAR2 in segments of small intestine from GF and CONV-R mice (n = 7 or 8 mice per group). **b**, PECAM-1 staining (red) of sections of small intestine from wild-type (WT), *F2r*$^{-/-}$ and *F2rl1*$^{-/-}$ mice. Nuclei were stained with Hoechst nuclear dye (blue). **c**, Quantification of **b** (n = 6–9 mice per group). **d**, **e**, Relative levels of mRNA for PECAM-1 (**d**) and Ang-1 (**e**) in segments of small intestine from wild-type, *F2r*$^{-/-}$ and *F2rl1*$^{-/-}$ mice (n = 6–9 mice per group). **f**, **g**, Anti-TF and anti-phospho-TF immunoblots of small-intestinal lysates from (**f**) WT, *F2r*$^{-/-}$ and *F2rl1*$^{-/-}$ miceand (**g**) CONV-D mice treated with PBS (control) or hirudin (1 mg/mouse) immediately before colonization and at 2 h and 4 h after colonization. **h**, Quantification of the phospho-TF band shown in **g** (n = 6 or 7 mice per group). **i**, Anti-TF and anti-phospho-TF immunoblots of primary enterocytes (from CONV-R mice) incubated for 2 h with human thrombin (50 nmol l^{-1}). **j**, Quantification of the phospho-TF band shown in **i** (n = 8 mice per group). Female Swiss Webster mice were analysed in **a** and **g–j**. Female WT, *F2r*$^{-/-}$ and *F2rl1*$^{-/-}$ mice on a C57BL6/J genetic background were used in **b–f**. Scale bars, 20 μm. Results are shown as means ± s.e.m. Asterisk, $P < 0.05$; three asterisks, $P < 0.005$; n.s., not significant.